


# Phytomolecules-Coated NiO Nanoparticles Synthesis Using *Abutilon indicum* Leaf Extract: Antioxidant, Antibacterial, and Anticancer Activities

This article was published in the following Dove Press journal:  
*International Journal of Nanomedicine*

Shakeel Ahmad Khan <sup>1</sup>  
Sammia Shahid<sup>2</sup>  
Amber Ayaz<sup>2</sup>  
Jawaher Alkahtani<sup>3</sup>  
Mohamed S Elshikh<sup>3</sup>  
Tauheeda Riaz<sup>4</sup>

<sup>1</sup>Center of Super-Diamond and Advanced Films (COSDAF) and Department of Chemistry, City University of Hong Kong, Kowloon, 999077, Hong Kong;

<sup>2</sup>Department of Chemistry, School of Science, University of Management and Technology, Lahore, 54770, Pakistan;

<sup>3</sup>Department of Botany and Microbiology, College of Science, King Saud University, Riyadh, 11451, Saudi Arabia;

<sup>4</sup>Department of Chemistry, Government College Women University Sialkot, Sialkot, Pakistan

**Background:** NiO nanoparticles have attracted much attention due to their unique properties. They have been synthesized using chemical and physical techniques that often need toxic chemicals. These toxic chemicals cannot easily be removed from the nanoparticle's surface, make them less biocompatible, and limit their biological applications. Instead, plants based green synthesis of nanoparticles uses phytomolecules as reducing and capping agents. These phytomolecules are biologically active with no or less toxic effects.

**Materials and Methods:** Phytomolecules-coated NiO nanoparticles were synthesized employing a green route using *Abutilon indicum* leaf extract. For comparative study, we also have synthesized NiO nanoparticles using the co-precipitation method. Synthesized nanoparticles were successfully characterized using different spectroscopic techniques. The synthesized nanoparticles were evaluated for antibacterial activity with agar well diffusion assay against different bacteria compared to standard drug and plant extract. They are also examined for anticancer potential using MTT assay against HeLa cancer cells, and further, their antioxidant potential was determined using DPPH assay. Biocompatibility of the synthesized nanoparticles was assessed against fibroblast cells.

**Results:** Phytomolecules-coated NiO nanoparticles were demonstrated superior antibacterial and anticancer performance against bacteria (*E. coli*, *B. bronchiseptica*, *B. subtilis*, and *S. aureus*) by presenting highest zone of inhibitions ( $18 \pm 0.58$  mm,  $21 \pm 0.45$  mm,  $22 \pm 0.32$  mm, and  $23 \pm 0.77$  mm) and HeLa cancer cells by exhibiting the least cell viability percentage ( $51.74 \pm 0.35\%$ ) compared to plant extract and chemically synthesized NiO nanoparticles but were comparable to standard antibiotic and anticancer drugs, respectively. Phytomolecules-coated NiO nanoparticles were also demonstrated excellent antioxidant activity ( $79.87 \pm 0.43\%$  DPPH inhibition) and biocompatibility ( $> 90\%$  cell viability) with fibroblast cells.

**Conclusion:** Nanoparticle synthesis using the *Abutilon indicum* leaf extract is an efficient and economical method, produces biocompatible and more biologically active nanoparticles, which can be an excellent candidate for therapeutic applications.

**Keywords:** NiO nanoparticles, green synthesis, *A. indicum*, biological, anticancer, antibacterial

## Introduction

Currently, multidrug resistance (MDR) pathogenic bacteria have become a severe issue globally, and they are considered a significant cause of fatalities, about 700,000 deaths per year.<sup>1</sup> This number can be projected to 10 million deaths

Correspondence: Shakeel Ahmad Khan  
Email shakilahmad56@gmail.com

per year if the current use of antibiotics continues.<sup>2</sup> MDR bacterial infections are severely impacting healthcare and preventive practices. Thus, it is obligatory to find out new alternatives to combat these MDR pathogenic bacteria.<sup>3–5</sup> Besides, cancer is also one of the significant causes of death in human beings, and the burden of cancer patients has doubled from 1975 to 2000.<sup>6</sup> In 2018, over 18 million cancer cases and 9.6 million fatalities due to this disease were reported.<sup>7</sup> It is estimated that cancer cases will be more than 29.5 million by 2040.<sup>8</sup> Several advancements in molecular and cellular biology have taken place for treating the cancer disease through chemotherapy, but it also poses numerous side effects on cancer patients besides positive ones.<sup>9</sup> Therefore, it is essential to develop new anticancer drugs with improved efficacy, biocompatibility, and minimum side effects.

In this instance, metal and metal oxide nanoparticles have gained much attention.<sup>10–14</sup> They are considered most opportunistic and worthwhile because of their unique physical properties such as light-absorbing properties, large surface area to volume ratio, smaller size, surface plasmon resonance, etc.<sup>9,15</sup> With nanometer size, the nanoparticles can easily be penetrated the cell wall of the pathogenic MDR bacteria compared to conventional antibiotics, which is the most important and influential factor for their excellent antibacterial activity. Moreover, metal and metal oxide nanoparticles also have the capability to induce oxidative stress by generating reactive oxygen species (ROS) after penetrating cancerous cells, which leads the cells to demise.<sup>16–19</sup> Based on these properties, they have been extensively utilized for their biomedicine applications (antidiabetic, drug-delivery, antilarvicidal, anticancer, antioxidant, antibacterial, antifungal, etc.), biosensing (glucose, potassium ion, nitrite, etc.), photocatalysis, and memory storage devices.<sup>20–24</sup> However, NiO nanoparticles have attained great interest due to their unique properties (electron transfer ability, supper conductance, electrocatalysis, high chemical and thermal stability, antibacterial, antifungal, anti-inflammatory, etc.). NiO nanoparticles are environmentally active material as they have a wide band-gap (3.6–4.0 eV) and can be used for the adsorption and photocatalysis of heavy metals and synthetic dyes, respectively.<sup>25–27</sup>

The nanoparticles are mostly synthesized using physical and chemical techniques; however, both these techniques are not easily scalable, demands more energy and hazardous chemical substances for reduction and capping.<sup>12</sup> The use of toxic chemicals for capping in

these techniques compromises the nanoparticle's biocompatibility and limits their biomedical applications.<sup>16</sup> Consequently, the nanoparticle synthesis employing biological techniques, specifically plant-based, is considered an alternate, economical, fast, easily scalable, more biocompatible, and worthwhile approach over the chemical and physical techniques.<sup>16,28–30</sup> Plant's based biological methods do not require toxic chemical substances as they used plant's phytochemicals (polyphenols, alkaloids, terpenoids, saponins, etc.) as reducing and capping agents for the nanoparticle's synthesis.<sup>31</sup>

Different plants and their other parts, such as stem, leaves, flowers, seeds, shoots, etc., have been widely utilized to synthesize several kinds of nanoparticles.<sup>9,15,16,20,21</sup> Some of these plants are biologically active but have serious biocompatibility issues, and some are not biologically active. For example, many researchers have used Stevia leaf extract for different nanoparticle synthesis. But in 2019, leaves and crude extracts of this plant were included in an FDA import alert with concerns about their safety for use in foods or supplements and potential for toxicity.<sup>32</sup> Therefore, nanoparticles for biological applications must be needed to be synthesized with such plants that have no biocompatibility issue, and they should also be biologically active. In this regard, *Abutilon indicum* has significant importance as this plant is biologically active and has no biocompatibility issues. *Abutilon indicum* is a medicinal plant and extensively utilized for the treatment of different types of diseases, including blood dysentery, allergy, bronchitis, pulmonary tuberculosis, mumps, rheumatism, diarrhea, vaginal infections, cleaning wounds and ulcers, relieving thirst, piles, jaundice, urinary disease, and leprosy since ancient times.<sup>33</sup> *Abutilon indicum* has numerous natural products, including flavonoids, phenolic acids, alkaloids, saponins, terpenoids, etc., that enable this plant to show different biological activities (analgesic,<sup>34</sup> anti-inflammatory,<sup>35</sup> antidiabetic,<sup>36</sup> antioxidant,<sup>37</sup> antimicrobial,<sup>38</sup> anticancer,<sup>39</sup> hepatoprotective,<sup>40</sup> anti-asthmatic,<sup>41</sup> antilarvicidal,<sup>42</sup> etc.). Herein, we have synthesized the phytochemicals-coated NiO nanoparticles using the leaves extract of *Abutilon indicum* first time as per the author's best knowledge. For comparative study, we also chemically synthesized the NiO nanoparticles with the coprecipitation method. The chemically synthesized and phytochemicals-coated NiO nanoparticles were further applied to evaluate their antioxidant, antibacterial, and anticancer activities.

## Materials and Methods

All the chemicals (analytical grade) and double staining kit were purchased from Sigma-Aldrich, Germany. The four bacterial strains (*B. subtilis* ATCC<sup>®</sup>19659<sup>™</sup>, *S. aureus* ATCC<sup>®</sup>6538<sup>™</sup>, *B. bronchiseptica* ATCC<sup>®</sup>10580<sup>™</sup>, and *E. coli* ATCC<sup>®</sup>25922<sup>™</sup>) were acquired from Pakistan Chemical Scientific Industrial Research Center (PCSIR), Lahore, Pakistan.

## Plant Material Collection and Extract Preparation

The fresh *Abutilon indicum* leaves were collected from a graveyard near old Anarkali, Lahore, Pakistan. The leaves of *Abutilon indicum* were washed with deionized (DI) water and shade dried for one month. The dried leaves were then ground into powder using a commercial grinder (Figure 1). The plant leaves powder was stored in glass bottles for future use.

The 20 g of leaves powder was taken in a 500 mL beaker, and then methanol (120 mL) and DI water (180 mL) were added. Subsequently, the reaction mixture was heated at 50 °C for 60 min with continuous stirring. After, the reaction mixture was set aside overnight by covering the beaker with aluminum foil. The reaction

mixture was then filtered with filter paper to remove the residues of the plant's leaves powder (Figure 1). Finally, the obtained leaf extract was stored in a glass bottle and stored in the refrigerator at 4 °C for further use.

## Synthesis of Phytomolecules-Coated NiO Nanoparticles

The leaf extract's 150 mL was taken in a 500 mL beaker, and subsequently, 3 g of Ni(NO<sub>3</sub>)<sub>2</sub>·6H<sub>2</sub>O was added. After, the ethylene glycol (1.5 mL) was added into the reaction mixture and stirred continuously until complete mixing (20 min) at 30 °C (Figure 1). In another beaker, 150 mL leaves extract was added, and subsequently, 3 g citric acid was then transferred in it and stirred for 60 min at 30 °C. After, both solutions were mixed, and the resultant reaction mixture was stirred continuously at 30 °C for 60 min to obtain the greenish color dispersion of NiO nanoparticles (Figure 1). After the filtration with filter paper, the obtained phytomolecules-coated NiO nanoparticles were washed using DI H<sub>2</sub>O thrice times and dehydrated overnight at 80 °C and then calcinated at 500 °C for 120 min. Finally, the black color phytomolecules-coated NiO nanoparticles were obtained and transferred in a glass bottle, and stored for further use.

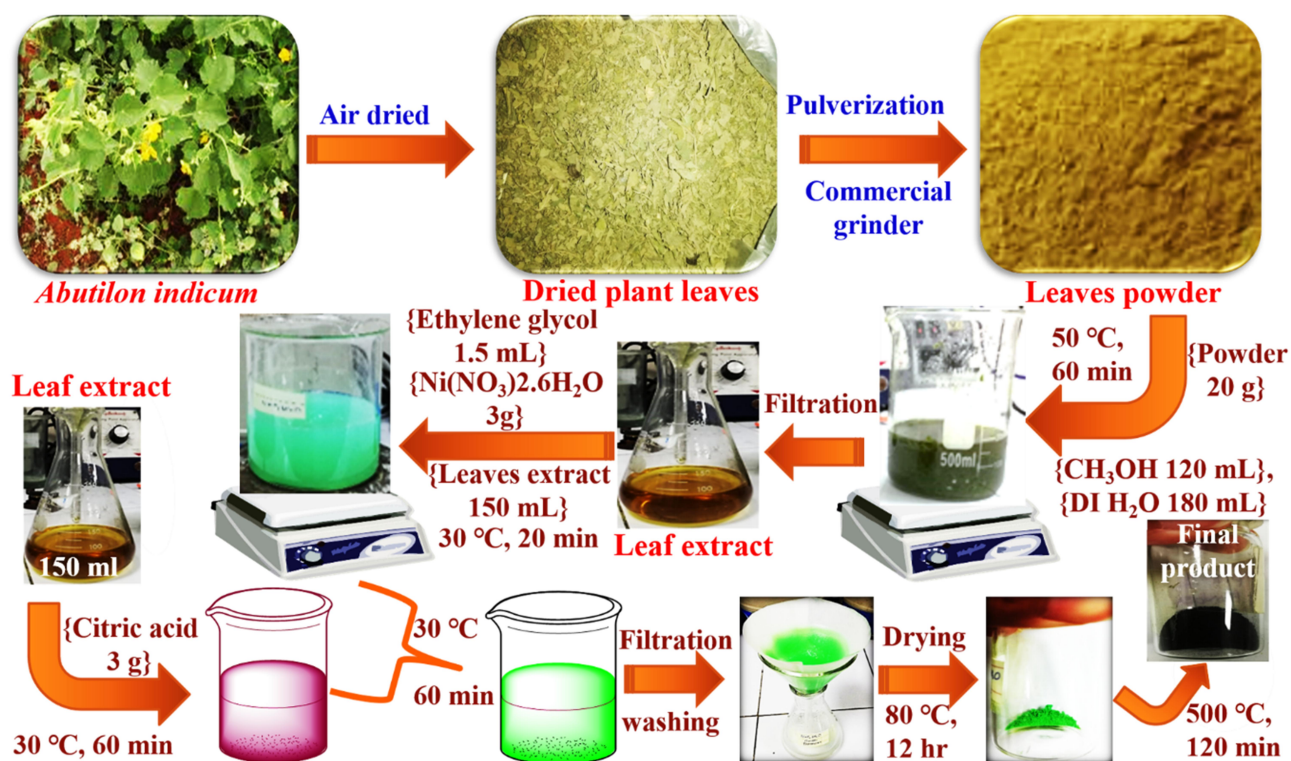


**Figure 1** The scheme for the green synthesis of phytomolecules-coated NiO nanoparticles using *Abutilon indicum* leaves extract.

## Synthesis of NiO Nanoparticles with Co-Precipitation Method

Ni(NO<sub>3</sub>)<sub>2</sub>·6H<sub>2</sub>O and NaOH were used as a precursor for synthesizing the NiO nanoparticles with the co-precipitation method. In brief, a 0.1 M solution of Ni salts and a 0.8 M solution of NaOH was prepared separately in DI water. After the NaOH solution was added dropwise into the Ni salts solution within 30 min, the subsequent resultant solution was further stirred at 80–85 °C for 6 hrs. Finally, the green color precipitates were formed, washed with ethanol and DI water thrice times. The precipitates were placed in an oven at 120 °C for drying. The obtained NiO nanoparticles were further annealed at 550–600 °C for 6 hr, and finally, black colored chemically synthesized NiO nanoparticles were obtained. They were stored in an airtight container for further use.

## Characterization

### X-Ray Diffraction Analysis

The crystallinity and purity of the green and chemically synthesized NiO nanoparticles in powder form were determined using the powder X-ray diffraction (XRD) (Bruker D2 PHASER with LYNXEYE XE-T detector, Haidian, Beijing, China) with a wavelength ( $\lambda$ ) of 0.154 nm over the 2 $\theta$  range 4–90°.

### Scanning Electron Microscope (SEM) and Energy-Dispersive X-Ray (EDX) Spectroscopy

The synthesized nanoparticles' morphology was characterized using an SEM (Quattro S) by placing the dried powder sample on the carbon tape. The compositional analysis was carried out with an energy-dispersive X-ray (EDX) spectroscopy using Thermo Fisher Scientific Ultradry (Madison, WI, USA) attached with SEM.

### Zetasizer Dynamic Light Scattering (DLS)

The green and chemically synthesized NiO nanoparticles were dissolved in DI water and sonicated for 5 min at 25–30 °C. About 10 mm sample solution was taken out and placed on a glass cuvette. After that, the cuvette was placed in the cell holder, and scanning was performed using a dynamic light scattering particle size analyzer (Malvern Zetasizer Nano ZS, Worcestershire, WR14 1XZ, UK) from 1 to 500 nm at 25–30 °C.

### UV-Visible Spectrophotometric Analysis

The green and chemically synthesized NiO nanoparticles were dissolved in DI water and sonicated for 5 min at 25–30 °C. The nanoparticles solution and plant extract

were then transferred in a quartz cuvette, and after being placed in the cell, the absorption maxima were determined from 200 to 800 nm using a UV-Visible spectrophotometer (Shimadzu 1700, Columbia, Maryland, USA) at 25–30 °C.

### Fourier Transform Infrared (FTIR) Analysis

The dried powder of green synthesized NiO nanoparticles and plant extract was placed on the quartz slide. The FTIR spectrum was measured from 450 to 4000 using Perkin Elmer Spectrum 100 spectrophotometer (Bridgeport Avenue Shelton, CT 06484–4794, USA) at 25–30 °C.

### Antibacterial Activity Evaluation

The antibacterial propensity of the phytomolecules-coated NiO nanoparticles was assessed against four bacterial strains (*B. subtilis*, *S. aureus*, *B. bronchiseptica*, and *E. coli*) compared to Leflox (antibiotic drug) and plant extract following the agar well diffusion method.<sup>43</sup> In a typical procedure, each sample solution of different concentrations such as 10 mg/mL, 20 mg/mL, 30 mg/mL, and 40 mg/mL was prepared in DI water by sonicating for 10 min to ensure uniform dispersion. After, 35 mL nutrient agar was added in petri dishes (diameter  $\times$  H = 90 mm  $\times$  15 mm, dish capacity  $\sim$ 90 mL), and subsequently, inoculum (3 mL) of each bacterial strain was transferred. The inoculum of each bacteria strain was prepared at  $1 \times 10^8$  CFU/mL. The petri plates were then set aside for 15 to 20 min to solidify the molten nutrient agar. After, the four holes of 4 mm in diameter were created in each petri dish with a pasteurized hollow-iron rod. The holes were then filled with 50  $\mu$ L of each sample solution (phytomolecules-coated NiO nanoparticles, plant extract, and standard drug) and kept on a flat surface for 1 hr. The petri dishes were then incubated at 37 °C for 24 hr. Each sample's antibacterial activity was then determined based on the appearance of zones of inhibitions (ZOIs) in the petri dish, and ZOIs were measured with the Vernier caliper.

### Cytotoxic Activity

The anticancer activity of the phytomolecules-coated NiO nanoparticles compared to the standard anticancer drug (doxorubicin) and plant extract was determined with the MTT colorimetric method against the HeLa cancer cells (Sigma-Aldrich, Germany).<sup>44</sup> The Cell Proliferation Kit I (MTT) was used for cytotoxic analysis. In brief, HeLa melanoma cells were added into 96 microtiter well plate, and 150  $\mu$ L DMEM was added, and the well plate was



then incubated at 37 °C for 24 hr to obtain cell density  $5 \times 10^8$  cells/well (cell's confluency was 75–80% measured by trypan blue-stained cells using a hemocytometer). Each sample solution (phytomolecules-coated NiO nanoparticles, standard drug, and plant extract) was prepared in DI water at different concentration levels (1, 5, 10, 15, 30, 60, and 120  $\mu\text{g/mL}$ ). After, 10  $\mu\text{L}$  of each sample solution was separately transferred to each well and again re-incubated for 24 hr at 37 °C. The cells were then centrifuged to remove supernatant and washed times thrice with phosphate buffer saline (PBS). The 100  $\mu\text{L}$  of MTT reagent (0.6 mg/mL) was transferred to each well and again re-incubated for 4 hr at 37 °C, and then DMSO (100  $\mu\text{L}$ ) was transferred to each well for solubilizing the undissolved formazan's crystals. After the plate was placed on the agitator for 15 min and then using the Varian Eclipse spectrophotometer, the absorption-maxima of formazans at 570 nm was measured. The cell cytotoxicity percentage was measured with the following equation;

$$\% \text{ Cell viability} = (\text{OD}_{\text{sample}}/\text{OD}_{\text{control}}) \times 100,$$

Where  $\text{OD}_{\text{control}}$  is referred for the cancer cells without any treatment and only served with media. The  $\text{OD}_{\text{sample}}$  is referred for the cancer cells treated with different samples' concentrations (phytomolecules-coated NiO nanoparticles, chemically synthesized NiO nanoparticles, an anticancer drug, and plant extract).

### Live/Dead Staining Assay

We investigated the HeLa cancer cell viability with the fluorescent staining technique to further affirm the cytotoxicity using the live/dead double staining kit (viable cells stain with green and dead cells with red). The same experiment repeated as described above till cancer cells treated with different samples (10  $\mu\text{L}$  of 120  $\mu\text{g/mL}$ ) and subsequent incubation. After, the staining solution (4  $\mu\text{g/mL}$ ) was added to each well at 37 °C and incubated for 20 min. The photographs were taken with an Olympus BX53 fluorescence microscope (excitation wavelength 488/545 nm for viable/dead cells).

### Antioxidant Activity in Terms of DPPH Percentage Inhibition Assay

The phytomolecules-coated NiO nanoparticles' antioxidant activity was determined by scavenging the DPPH free radical compared to plant extract, chemically synthesized NiO nanoparticles, and external standard butylated hydroxytoluene (BHT) via the protocol previously described by Khan et al.<sup>16</sup> In brief, DPPH solution of 0.1

mM and each sample's solution with different concentrations (25, 50, 75, and 100  $\mu\text{g/mL}$ ) was separately prepared in ethanol and DI water, respectively. Afterward, each sample's solution was individually mixed with a DPPH solution. The resultant reaction mixtures were stirred for 10 min at 30 °C and set aside for 24 hr. The antioxidant activity in terms of DPPH percentage inhibition was then determined using a UV-Visible spectrophotometer at 517 nm. The DPPH percentage inhibition was calculated by using the following equation:

$$\text{DPPH percentage inhibition} = [(A_c - A_s)/A_c] \times 100$$

where,  $A_s$  is the absorbance of the sample, and  $A_c$  is the absorbance of the control (only DPPH solution).

### Antioxidant Activity in Terms of Linoleic Acid (%) Inhibition

The antioxidant potential of phytomolecules-coated NiO nanoparticles in terms of linoleic acid (%) inhibition was determined in comparison to plant extracts and chemically synthesized NiO nanoparticles, following the protocol reported by Khan et al.<sup>45</sup> In detail, 100  $\mu\text{g/mL}$  concentration of each sample was added to the solution mixture of 0.2 M sodium phosphate buffer (pH 7.0, 10 mL), 99.99% ethanol (10 mL), and linoleic acid (0.13 mL). The resulting solution's total volume was made up to 25 mL with DI water and subsequently incubated for 360 hrs at 40 °C. The extent of oxidation was measured using the thiocyanate method. Accordingly, 0.2 mL of the sample solution was taken and then added to 10 mL of ethanol (75%). Subsequently, 0.2 mL of aqueous ammonium thiocyanate solution (30%) and 0.2 mL  $\text{FeCl}_2$  (20 mM in 3.5% HCl) was added. The reaction mixture was stirred for 3 min, and the absorption maxima were then measured at 500 nm wavelength. The percentage inhibition of linoleic acid was calculated using the following formula:

$$\% \text{ Inhibition} = [100 - (\text{Absorbance of sample})/(\text{absorbance of control})] \times 100$$

The Butylated hydroxytoluene was used as an external standard, and the control only consisted of linoleic acid without any treatment.

### Biocompatibility Evaluation

The biocompatibility of the phytomolecules-coated NiO nanoparticles against the Human foreskin fibroblasts cells was evaluated compared to chemically synthesized NiO nanoparticles and plant extract via the standard protocol reported by Hoyo et al.<sup>46</sup> The fibroblasts cells were maintained in 4 ppm of DMEM (Dulbecco's Modified Eagle

Medium) for 24 hr at 37 °C temperature in a humidified atmosphere with 5% CO<sub>2</sub>. The cells at pre-confluence were harvested in trypsin-EDTA (ATCC-30-2101) and then seeded on a 24-well microtiter plate at the cell's density of 1.0×10<sup>5</sup> cells per well for 24 hr at 37 °C. The cells were then washed using PBS. After the 50 µL of each sample's solution at 120 µg/mL were immersed in each well separately, and 1 mL of DMEM was added in each well. The 24-well microtiter plate was then incubated for 24 hr at 37 °C. The cells were then stained with AlamarBlue (100 µL, 10% v/v) at 37 °C for 4 hr. Finally, the cell viability was calculated by measuring the optical density (OD) at the absorbance of 570 nm using a microplate reader:

$$\text{Cell viability (\%)} = (\text{OD value of treated cells}) / (\text{OD value of control}) \times 100$$

### Live/Dead Staining Assay

To further affirm the biocompatibility, we investigated the fibroblasts cells viability with fluorescent staining technique using the live/dead double staining kit (viable cells stains with green and dead cells with red). The same experiment repeated as reported by<sup>46</sup> till fibroblasts cells were treated with different samples (10 µL of 120 µg/mL) and subsequent incubation. After, the staining solution (4 µg/mL) was added to each well at 37 °C and incubated for 20 min. The photographs were taken with an Olympus BX53 fluorescence microscope (excitation wavelength 488/545 nm for viable/dead cells).

### Statistical Analysis

All the experiments (antibacterial, anticancer, antioxidant, and biocompatibility) were conducted three times, and the results are presented as mean ± standard deviation. One-way ANOVA at a fixed significance level (0.05) and Tukey's test were also applied to the results to determine the significance.

## Results and Discussion

### Synthesis Mechanism

Many reports state that different parts (leaves, roots, fruits, and flower) of *Abutilon indicum* is a rich source of several biologically active phytochemical constituents, including phenolics, tannins, starch, glycosides, flavonoids, alkaloids, steroids, and carbohydrates compounds. Due to the presence of these natural products, *Abutilon indicum* has been extensively used for treating numerous types of ailments (blood dysentery, allergy, bronchitis, pulmonary tuberculosis, mumps, rheumatism, diarrhea, vaginal

infections, cleaning wounds, and ulcers, relieving thirst, piles, jaundice, urinary disease, etc.) in traditional medicine.<sup>47,48</sup>

In one study by GC-MS, Saranya et al have reported the triamcinolone acetonide, hydroxybenzoic acid ester, arabinitol pentaacetate, 5-thio-D-glucose, abutilin A, Z-11-hexadecenoic acid, 3-hydroxy-beta-ionol, 10-methoxydihydrocorynantheol, 10-methoxycorynan-17-ol, etc. in the leaves extract of *Abutilon indicum*.<sup>49</sup> Moreover, Kuo et al have isolated the thirty compounds (β-sitosterol and stigmasterol, vanillin, methylcoumarate, 4-hydroxyacetophenone, p-hydroxybenzaldehyde, auran-tiamide acetate, methyl indole-3-carboxylate, 3,7-dihydroxychromen-2-one, methylparaben, scoparone, scopoletin, syringaldehyde, 1-methoxycarbonyl-β-carboline, 4-hydroxy-3-methoxy-trans-cinnamic acid methyl ester, trans-p-coumaric acid, thymine, adenine, methyl 4-hydroxyphenylacetate, riboflavin, 1-lycoperodine, 3-hydroxy-β-damascone, adenosine, p-hydroxybenzoic acid, 3-hydroxy-β-ionol, N-feruloyl tyrosine, vanillic acid, and benzoic acid) from the extract of *Abutilon indicum*.<sup>50</sup> Therefore, due to these phytochemicals, leaves extract of *Abutilon indicum* can be performed role as reducing and capping agents. In phytochemicals-coated NiO nanoparticles synthesis, the nickel salt first ionizes into its respective ions (Ni<sup>2+</sup>) in the presence of leaves extract (Figure 2). Phytochemicals (starch, glycosides, flavonoids, carbohydrates, polyphenols, etc.) of leaves extract readily reduce the metallic ions of nickel to metallic oxide nanoparticles (NiO) through redox reaction, as shown in Figure 2. Further, once NiO nanoparticles are formed, the phytochemicals (tannins, alkaloids, steroids, proteins, etc.) stabilize and capped them (Figure 2). The capping and adsorption of these phytochemicals on the surface of phytochemicals-coated NiO nanoparticles are also evident from the UV-Visible and FTIR spectra (Figure 3) that support our proposed synthesis mechanism.

### Characterization

#### UV-Visible Analysis

The absorption maxima of plant leaf extract, and phytochemicals-coated NiO nanoparticles were determined with a UV-Visible spectrophotometer. Figure 3A and B displays the UV-Visible spectra. The results reveal that *Abutilon indicum* leaves extract demonstrated the broad absorption spectrum in the UV-Visible region (200 to 385 nm), indicating the presence of flavonoids and polyphenolics compounds (Figure 3A). Reports show that these phytochemicals mostly



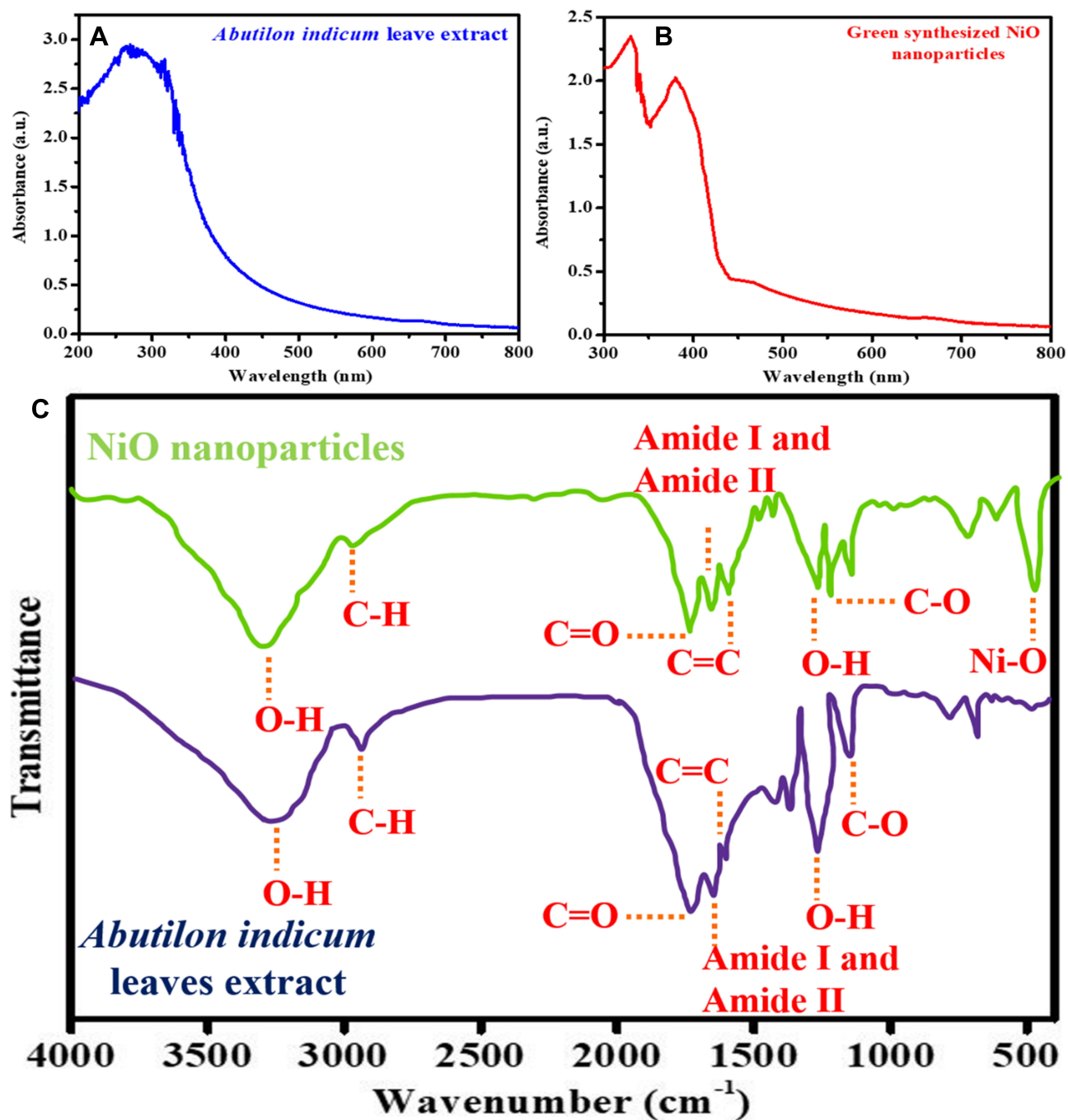


**Figure 3** UV-Visible spectra of (A) *Abutilon indicum* leaves extract, and (B) phytomolecules-coated NiO nanoparticles. (C) FTIR spectrum of *Abutilon indicum* leaves extract, and phytomolecules-coated NiO nanoparticles.

d orbitals, which further led to the electronic transition. The same redshift in absorption maxima was reported by Khan et al and Roy et al.<sup>9,52</sup>

#### FTIR Analysis

FTIR analysis was carried out to identify functional groups of phytomolecules responsible for synthesizing the

phytomolecules-coated NiO nanoparticles by acting as reducing and capping agents. Figure 3C shows the FTIR spectra of *Abutilon indicum* leaves extract and phytomolecules-coated NiO nanoparticles. The FTIR spectral results of leaves extract of *Abutilon indicum* displayed different peaks that were observed at 3410  $\text{cm}^{-1}$  (O-H), 2990  $\text{cm}^{-1}$  (C-H), 1702  $\text{cm}^{-1}$  (C=O), 1650  $\text{cm}^{-1}$  (amide I and amide II), 1630  $\text{cm}^{-1}$  (C=C),



1259  $\text{cm}^{-1}$  (O-H), 1140  $\text{cm}^{-1}$  (C-O). Similar FTIR signals for the leaves extract of *Abutilon indicum* were also stated by Khan et al, Singh et al, and Saranya et al.<sup>9,48,49</sup> On the other hand, the FTIR spectrum of the phytomolecules-coated NiO nanoparticles not only exhibited the peaks corresponding to Ni-O at 430  $\text{cm}^{-1}$  but also demonstrated the several FTIR signals that are attributed to the phytomolecules of the leaves extract of *Abutilon indicum*. Kannan et al were also reported similar FTIR signals for the Ni-O.<sup>51</sup> Thus, the FTIR results were corroborated the successful synthesis of phytomolecules-coated NiO nanoparticles that were capped with the biologically active plant's phytochemicals.

### XRD Analysis

Figure 4A and Figure S1A show the XRD spectrum of the phytomolecules-coated NiO and chemically synthesized NiO nanoparticles. The XRD pattern of phytomolecules-coated NiO nanoparticles displays the strong, sharp, and

intense peaks indexing to (111), (200), (220), (311), and (222) crystal plane at a diffraction angle of 37.25°, 43.26°, 63.11°, 75.46°, and 79.45° respectively. The XRD pattern further exhibited that phytomolecules-coated NiO nanoparticles are highly crystalline. Our phytomolecules-coated NiO nanoparticles' XRD pattern is well-matched with the JCPDS card No. 01-175-0269.<sup>53</sup> Ezhilarasi et al and Ramesh et al were also reported similar results.<sup>27,53</sup>

### SEM and Zeta Potential Studies

The morphologies of the phytomolecules-coated NiO nanoparticles and chemically synthesized NiO nanoparticles were determined using SEM. Figure 4B and Figure S1B show the SEM images of the green synthesized and chemically synthesized NiO nanoparticles, respectively. SEM results demonstrate that they are appropriately dispersed and highly crystalline and have cubic (green synthesized) and spherical (chemically synthesized)

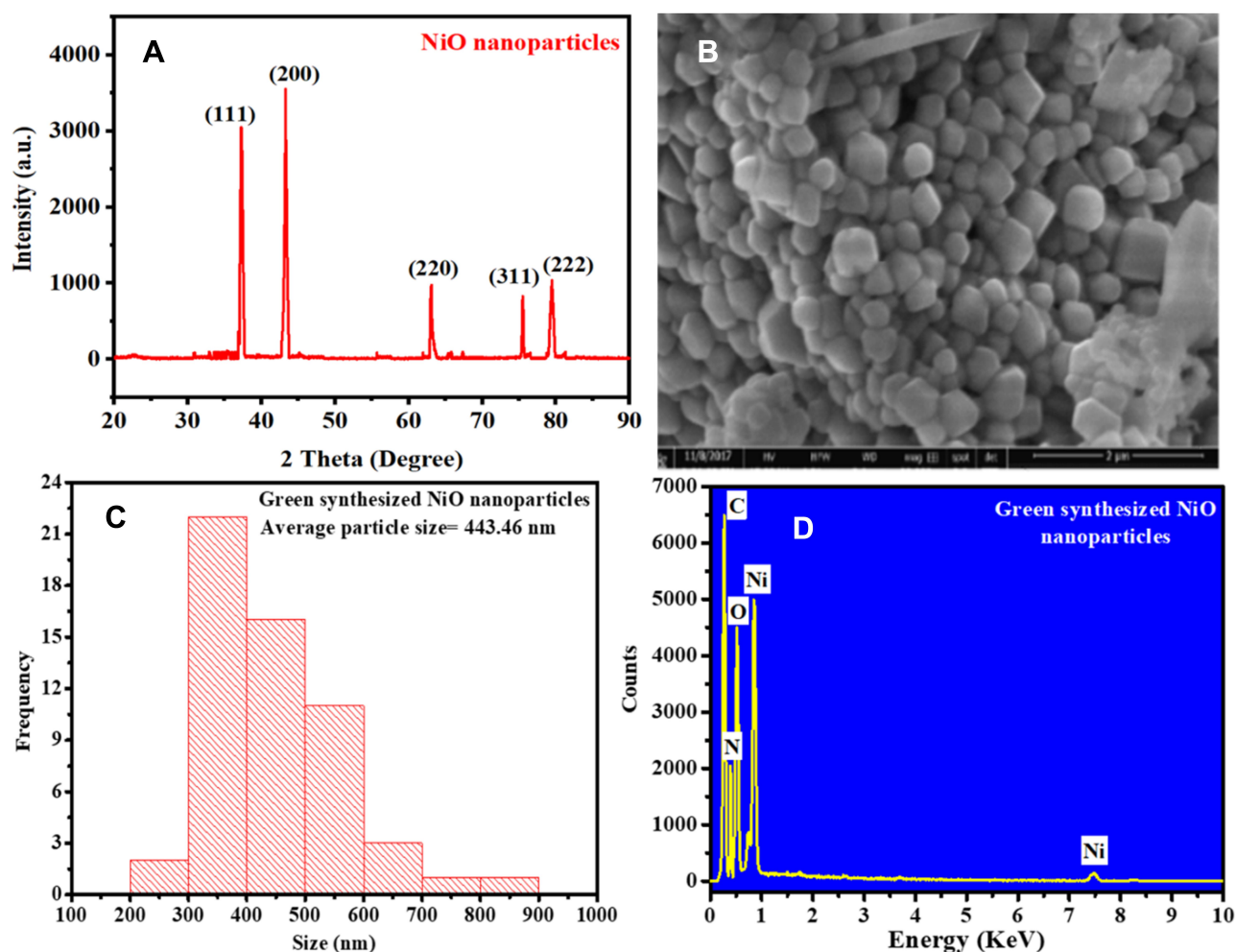


Figure 4 The (A) XRD, (B) SEM, (C) DLS particle size distribution, and (D) EDX of phytomolecules-coated NiO nanoparticles using *Abutilon indicum* leaves extract.

morphology.<sup>27,52</sup> Some of the synthesized nanoparticles are found agglomerated. The average nanoparticle sizes of chemically synthesized and phytomolecules-coated NiO nanoparticles measured by Zetasizer dynamic light scattering system were  $452.49 \pm 0.6$  nm (Figure S1C) and  $443.46 \pm 0.9$  nm (Figure 4C), respectively. The PDI value of green synthesized was observed 0.319, while for chemically synthesized, it was 0.215.

The stability of the chemically synthesized NiO nanoparticles and phytomolecules-coated NiO nanoparticles was determined by measuring their zeta potential. The stability of the nanoparticles is associated with more negative charges. The results indicated that the phytomolecules-coated NiO nanoparticles have  $-10.95$  mV zeta potential while chemically synthesized NiO nanoparticles have  $-18.50$  mV zeta potential. Similar zeta potential results were reported by Kumar et al for the chemically synthesized, and green synthesized NiO nanoparticles.<sup>54</sup>

### EDX Analysis

The compositional analysis of the phytomolecules-coated NiO nanoparticles and chemically synthesized NiO nanoparticles was carried out with EDX, and Figure 4D and Figure S1D show the EDX pattern, respectively. The EDX peaks at 0.85 KeV and 7.48 KeV are attributed to the presence of “Ni”.<sup>27,49</sup> While the peak at 0.52 KeV is indicated the presence of oxygen “O.” Thus, the presence of nickel and oxygen peaks in the EDX spectrum validated the successful synthesis of phytomolecules-coated NiO nanoparticles. Besides, two sharp and intense EDX peaks at 0.27 KeV and 0.392 KeV are also evident in the EDX pattern, which corresponds to the presence of carbon “C” and nitrogen “N,” respectively.<sup>27,31</sup> The carbon and nitrogen peaks might originate from the phytomolecules of plant’s leaves extract adsorbed on the surface of phytomolecules-coated NiO nanoparticles.

On the other hand, sharp nickel and oxygen EDX peaks are evident in the EDX pattern of the chemically synthesized NiO nanoparticles. The small EDX peak associated with carbon is also apparent in the EDX pattern, which might be attributed to the carbon tape signal that holds the nanoparticles, as shown in Figure S1D. Hence, EDX pattern results were corroborated that the phytomolecules-coated NiO nanoparticles of our interest have been successfully fabricated using *Abutilon indicum* leaves extract.

### Antibacterial Propensity

The antibacterial propensity of the phytomolecules-coated NiO nanoparticles was determined compared to the leaf

extract of *Abutilon indicum* and antibacterial drug (Leflox). Figures 5A–D and 6A shows the antibacterial propensity results in the form of ZOIs. The superior antibacterial performance was demonstrated by the phytomolecules-coated NiO nanoparticles at the concentration of 40 mg/mL against Gram-negative (*E. coli* and *B. bronchiseptica*) and Gram-positive (*B. subtilis* and *S. aureus*) bacteria by demonstrating the highest ZOIs ( $18 \pm 0.58$  mm,  $21 \pm 0.45$  mm,  $22 \pm 0.32$  mm, and  $23 \pm 0.77$  mm) respectively, compared to plant extract and chemically synthesized NiO nanoparticles at the same concentration level. The results also demonstrated that the antibacterial propensity of the phytomolecules-coated NiO nanoparticles was comparable to the standard antibiotic drug at all tested concentrations against the bacterial strains. It was interesting to note that leaves extract of *Abutilon indicum* also exhibited the inhibitory action against all the bacterial strains. This implies that the leaves extract has biologically active phytomolecules that have the ability to kill bacterial strains.<sup>9,37</sup> The nanoparticles, plant extract, and antibiotic drug were demonstrated the concentration-dependent antibacterial propensity.

Further, it was also observed that phytomolecules-coated NiO nanoparticles displayed excellent antibacterial performance against Gram-positive than Gram-negative bacterial strains. This might be due to the variances in the chemical structure of the cell wall of both the bacteria and further their different level of susceptibility towards metal oxide nanoparticles.<sup>27</sup> A similar more antibacterial effect of NiO nanoparticles towards Gram-positive than Gram-negative bacteria was also reported by previous studies.<sup>27,55</sup> Our phytomolecules-coated NiO nanoparticles displayed a more antibacterial effect compared to previously reported against *S. aureus*, *B. subtilis*, and *E. coli*.<sup>27,56</sup> This might be because of the adsorption of biologically active natural products of the *Abutilon indicum* leaves extract on NiO nanoparticles’ surface that was also participated along with nanoparticles (synergetic) to inhibit bacteria’s growth. The exact antibacterial mechanism of action of phytomolecules-coated NiO nanoparticles is still unclear. But many studies proposed that the phytomolecules-coated NiO nanoparticles in the solution release reactive radicals  $\text{Ni}^{2+}$  ions that get attached to the negatively charged cell wall of bacteria due to electrostatic force of attraction (Figure 6B). The strong adhesion of  $\text{Ni}^{2+}$  ions to the bacterial cells disrupts the cell membrane, leading the bacterial cell to demise.<sup>27,51,52,56</sup>

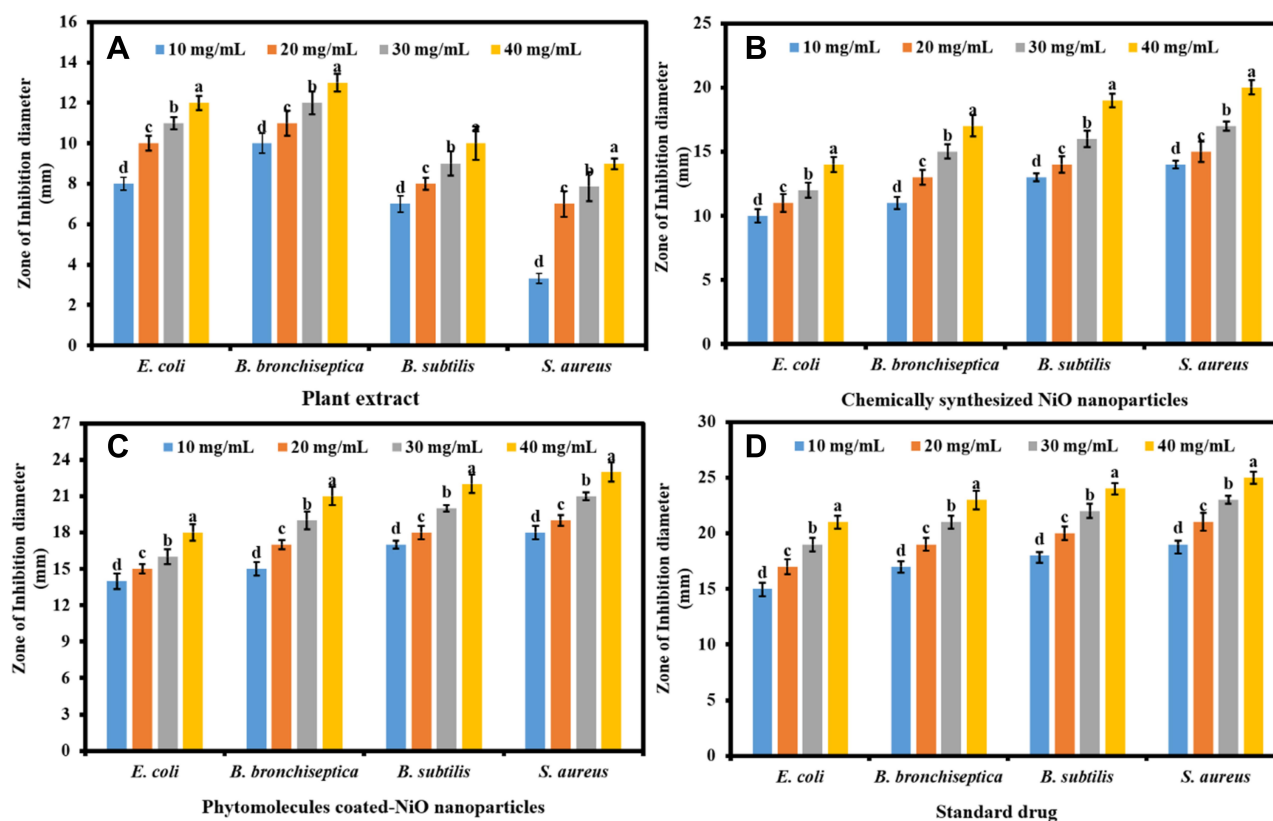


**Figure 5** The antibacterial propensity in terms of ZOI; (A) plant leaves extract, (B) chemically synthesized NiO nanoparticles, (C) phytomolecules-coated NiO nanoparticles ( $F = 1072.028$ ,  $p < 0.001$ ), and (D) antibacterial drug.

**Note:** Tukey based heterogeneous lower-case letters represent significant pairs.

## Anticancer Activity

The phytomolecules-coated NiO nanoparticles were evaluated for their anticancer potential against HeLa cancerous cell line compared to a plant extract and standard anticancer drug. Figure 7 shows the anticancer result in terms of cell viability percentage. Results of cell viability percentage were demonstrated that phytomolecules-coated NiO nanoparticles exhibited a significant cytotoxic effect on HeLa cancer cells compared to chemically synthesized NiO nanoparticles and leaves extract of *Abutilon indicum*. The cytotoxic effect of phytomolecules-coated NiO nanoparticles on HeLa cancer cells was comparable to standard anticancer drugs, and both presented more than 50% cytotoxicity. Moreover, results also showed that the plant's leaves extract exhibited good cytotoxicity, which revealed that it has such phytochemicals that are biologically active towards cancerous cells. Moreover, phytomolecules-coated NiO nanoparticles, plant extract, and anticancer drug were presented the concentration-dependent anticancer propensity against HeLa cancer cells, and the

maximum cytotoxic effect was observed with their 120  $\mu\text{g}/\text{mL}$  concentration.<sup>57–59</sup>

To observe the morphological changes in HeLa cancer cells after treatment with concentration 120  $\mu\text{g}/\text{mL}$  of plant extract, green synthesized NiO nanoparticles, and chemically synthesized NiO nanoparticles, we employed an inverted microscope (Nikon Eclipse TE200) and the results are displayed in Figure 8A–D. Results show that HeLa cancer cells endured severe morphological alterations, including reducing the cytoplasm and cell rounding.

We further investigated the HeLa cancer cell viability with the fluorescent staining technique to affirm the cytotoxicity, and the results are presented in Figure 8E–H. Live (Green)/dead (red) staining results demonstrated that the maximum cytotoxic effect on HeLa cancer cells appeared upon treatment with green synthesized NiO nanoparticles compared to plant extract and chemically synthesized NiO nanoparticles. These results are found consistent with the MTT assay and inverted microscopic results.

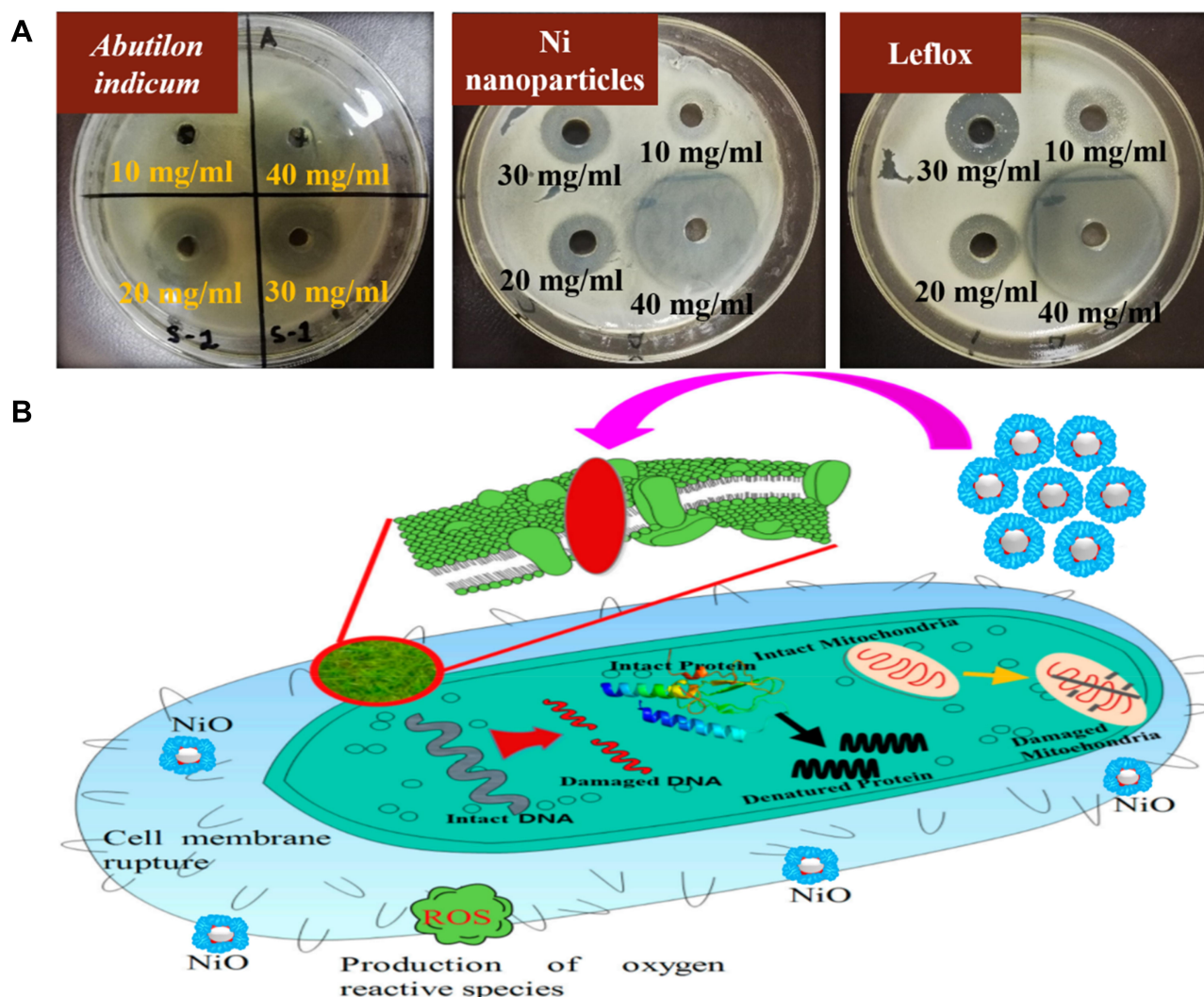


**Figure 6 (A)** The representative agar plates of *S. aureus* treated with plant extract, phytomolecules-coated NiO nanoparticles, and standard drug. **(B)** The probable antibacterial mechanism of the phytomolecules-coated NiO nanoparticles **Notes:** Adapted from Srihasam S, Thyagarajan K, Korivi M, Lebaka VR, Mallem SP. Phytogetic generation of NiO nanoparticles using Stevia leaf extract and evaluation of their in-vitro antioxidant and antimicrobial properties. *Biomolecules*. 2020;10(1):89. <sup>56</sup>

The remarkable anticancer propensity outcomes of the phytomolecules-coated NiO nanoparticles might be attributed to their physical properties (large surface area, morphology, and smaller particle size) and their surface's functionalization the biologically active phytochemicals of *Abutilon indicum* leaves extract. Reports demonstrate that *Abutilon indicum* leaves extract possesses molecular functionalities that have significant anticancer potential against different cancerous cells.<sup>9,38</sup> The enhanced anticancer results were reported with the green synthesized nanoparticles compared to nanoparticles prepared with other methods.<sup>60,61</sup> Hence, it can be concluded that nanoparticle's physical characteristics and functionalization with biologically active molecules have a significant role in enhancing the anticancer potential.

#### Antioxidant Activity in Terms of DPPH Percentage Inhibition

The antioxidant activity of the phytomolecules-coated NiO nanoparticles was evaluated by scavenging the DPPH free radicals. Results were indicated that all the tested samples displayed concentration-dependent antioxidant activity (Figure 9). The phytomolecules-coated NiO nanoparticles were presented the superior DPPH scavenging ability compared to plant extract and chemically synthesized NiO nanoparticles but slightly lower than standard (BHT). On the other hand, chemically synthesized NiO nanoparticles were demonstrated the least antioxidant activity. It was noteworthy that plant extract also exhibited good antioxidant activity by scavenging the DPPH. These results indicated that *Abutilon*



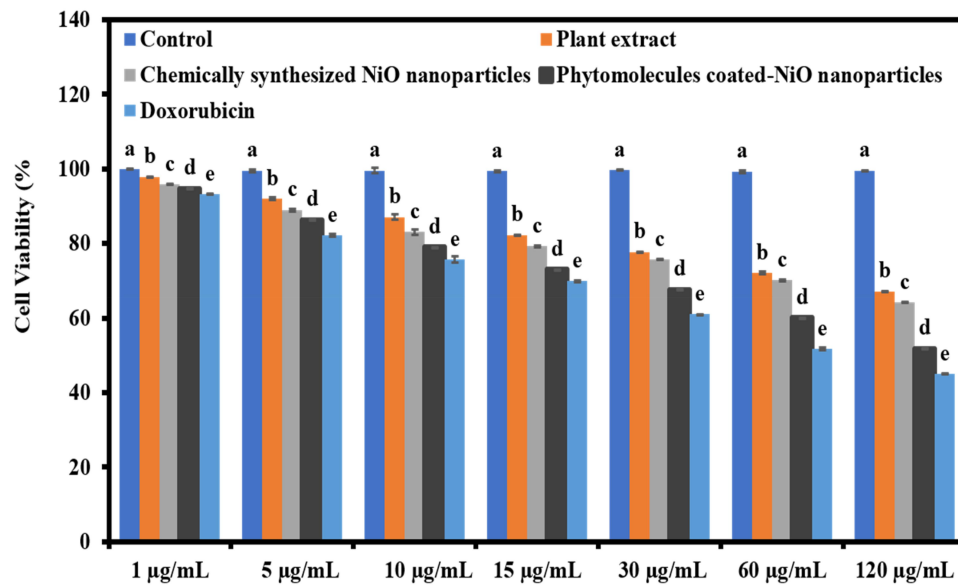


**Figure 7** The anticancer potential of phytomolecules-coated NiO nanoparticles compared to leaves extract of *Abutilon indicum*, chemically synthesized NiO nanoparticles, and standard drug in terms of cell viability percentage against HeLa cancer cells ( $F = 7225.663$ ,  $p < 0.001$ ).

**Note:** Tukey based heterogeneous lower-case letters represent significant pairs.

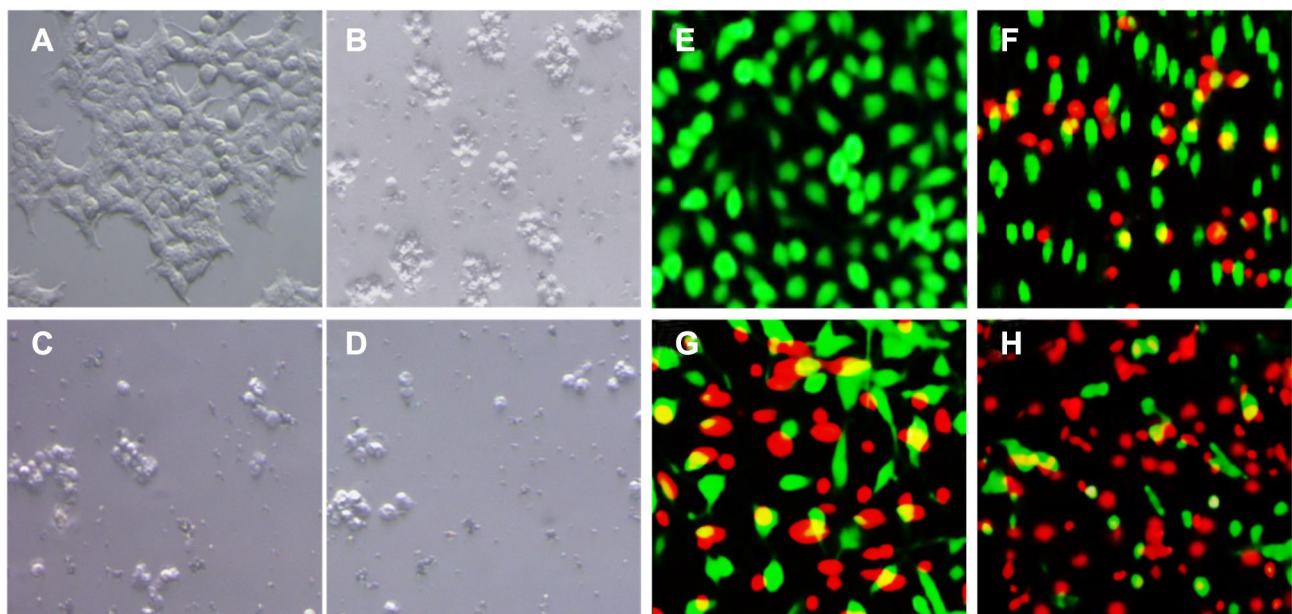


**Figure 8** The inverted micrographs of HeLa cells were incubated with (B) plant extract, (C) chemically synthesized NiO nanoparticles, and (D) phytomolecules-coated NiO nanoparticles. The fluorescence micrograph of live and dead HeLa cells incubated with (F) plant extract, (G) chemically synthesized NiO nanoparticles, and (H) phytomolecules-coated NiO nanoparticles. (A) and (E) control (scale bar, 100 µm).

*indicum* leaves extract is a rich source of natural antioxidants. Moreover, the superior antioxidant activity of the phytomolecules-coated NiO nanoparticles might be attributed to the presence of plant extract's phytomolecules (flavonoids, phenolic acids, alkaloids, etc.) on the surface of nanoparticles. Srihasam et al are also reported similar antioxidant results for the NiO Nanoparticles synthesized using stevia leaf extract.<sup>56</sup>

#### Antioxidant Activity in Terms of Linoleic Acid Peroxidation Inhibition

The antioxidant activity of the phytomolecules-coated NiO nanoparticles was further evaluated in terms of linoleic acid peroxidation inhibition compared to plant leaves extract, chemically synthesized NiO nanoparticles and commercial standard (BHT). Results were displayed that

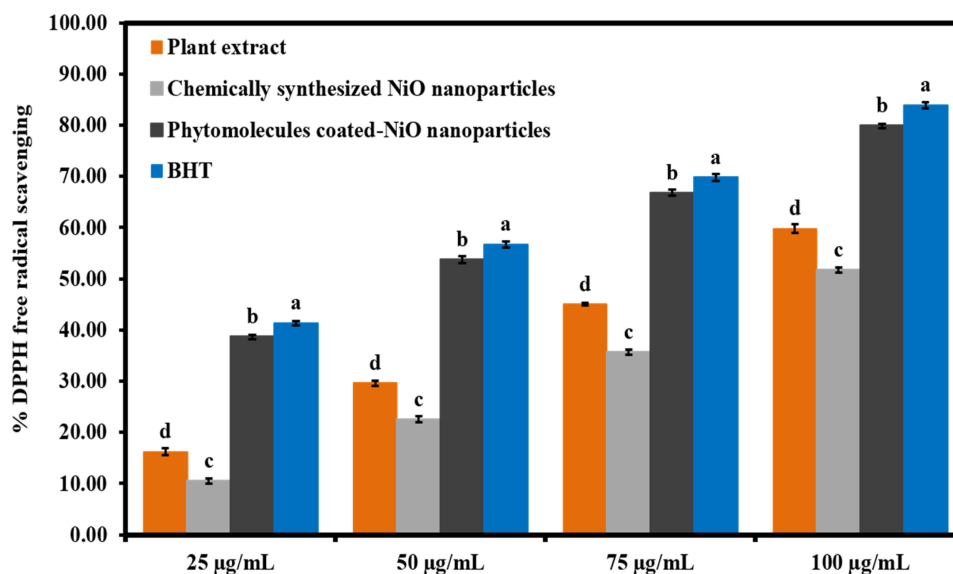


**Figure 9** The antioxidant activity results of phytomolecules-coated NiO nanoparticles in terms of %DPPH scavenging at different concentration levels than plant extract, chemically synthesized NiO nanoparticles, and BHT.

**Note:** Tukey based heterogeneous lower-case letters represent significant pairs.

the phytomolecules-coated NiO nanoparticles presented the superior linoleic acid peroxidation inhibition percentage ( $30.05 \pm 0.07\%$ ) compared to chemically synthesized NiO nanoparticles but slightly lower than plant extract and BHT (Figure S2). On the other hand, chemically synthesized NiO nanoparticles were demonstrated the least antioxidant activity ( $50.50 \pm 0.70\%$ ). These results indicated that *Abutilon indicum* leaves extract is a rich source of natural antioxidants. Moreover, the superior antioxidant activity of the phytomolecules-coated NiO nanoparticles compared to chemically synthesized NiO nanoparticles might be attributed to the presence of plant extract's phytomolecules (flavonoids, phenolic acids, alkaloids, etc.) on the surface of nanoparticles.

### Biocompatibility Studies

The biocompatibility of the phytomolecules-coated NiO nanoparticles was evaluated in vitro on fibroblast cells compared to plant leaves extract and chemically synthesized NiO nanoparticles, and the results are presented in the form of cell viability (%) as shown in Figure 10A. The results were demonstrated that the least cell viability percentage of fibroblast cells ( $80.46 \pm 0.31\%$ ) was observed with chemically synthesized NiO nanoparticles. On the other hand, phytomolecules-coated NiO nanoparticles were presented  $> 90\%$  cell viability (%) with the fibroblast cells. Moreover, it was interesting to note that plant leaves extract

has such phytochemicals that are biocompatible and exhibited excellent biocompatibility with the fibroblast cells.

To further confirm the biocompatibility, we investigated the fibroblast cells viability with the Live/dead fluorescent staining technique, and the results are displayed in Figure 10B–E. The results indicated that chemically synthesized NiO nanoparticles had pose more toxic effect on fibroblast cells as many dead cells (Red) appeared compared to plant extract and green synthesized NiO nanoparticles. The excellent biocompatibility of the phytomolecules-coated NiO nanoparticles might be attributed to the presence of different phytochemicals of plant's leaves extract on their surfaces. Henceforth, phytomolecules-coated NiO nanoparticles can be used for various biological applications. Both cell viability percentage results and staining assay results are found consistent with each other.

### Conclusions

In this work, phytomolecules-coated NiO nanoparticles were successfully synthesized, employing a green route using *Abutilon indicum* leaf extract as reducing and capping agents. The phytomolecules-coated NiO nanoparticles were characterized by FTIR, UV-Visible, XRD, SEM, and EDX. The phytomolecules-coated NiO nanoparticles synthesized using plant's leaves extract showed excellent antibacterial performance by inhibiting the growth of Gram-negative and Gram-positive bacterial strains compared to plant extract and chemically

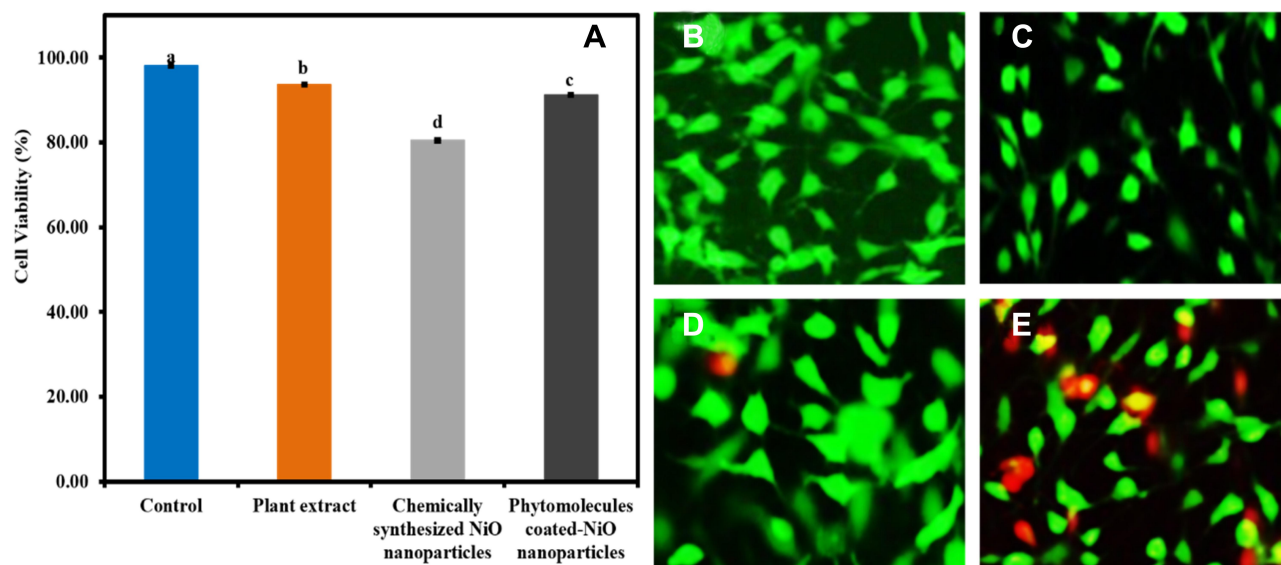


**Figure 10** (A) The biocompatibility results of phytomolecules-coated NiO nanoparticles with fibroblast cells compared to other tested samples (Note: Tukey based heterogeneous lower-case letters represent significant pairs). The fluorescence micrograph of live and dead fibroblast cells incubated with samples. (B) control, (C) plant extract, (D) green synthesized NiO, and (E) chemically synthesized NiO nanoparticles (scale bar 100  $\mu$ m).

synthesized NiO nanoparticles. However, they demonstrated comparable antibacterial activity compared to the standard antibiotic drug. The phytomolecules-coated NiO nanoparticles were further exhibited significant anticancer activity against the HeLa cancer cell lines, which was also comparable to the standard anticancer drug (Doxorubicin). The phytomolecules-coated NiO nanoparticles were also demonstrated excellent antioxidant activity and biocompatibility with fibroblast cells compared to chemically synthesized NiO nanoparticles. It was interesting to note that *Abutilon indicum* leaves extract was also found active towards antibacterial, antioxidant, and anticancer activities. Thus, antioxidant, antibacterial, and anticancer activities results displayed the potential of phytomolecules-coated NiO nanoparticles for their biomedical applications. Our results further recommended that phytomolecules-coated NiO nanoparticles exhibited excellent biological activities and biocompatibility due to the synergistic effect (physical properties and adsorbed phytomolecules on their surfaces). Hence, nanoparticles synthesis using leaf extract of *Abutilon indicum* is an efficient, robust, economical, and green method that produces biocompatible and biological active nanoparticles.

## Acknowledgments

Authors are very thankful to the Department of Chemistry, University of Management and Technology Lahore, Pakistan, for support of this research work. The authors

extend their appreciation to the Researchers Supporting Project number (RSP-2020/193) King Saud University, Riyadh, Saudi Arabia.

## Funding

This research was funded by King Saud University, Riyadh, Saudi Arabia, “grant number RSP-2020/193” and The APC was funded by “RSP-2020/193”.

## Disclosure

The authors declare no conflicts of interest in this work.

## References

- Galbadage T, Liu D, Alemany LB, et al. Molecular nanomachines disrupt bacterial cell wall, increasing sensitivity of extensively drug-resistant klebsiella pneumoniae to meropenem. *ACS Nano*. 2019;13(12):14377–14387. doi:10.1021/acsnano.9b07836
- Brown ED, Wright GD. Antibacterial drug discovery in the resistance era. *Nature*. 2016;529(7586):336–343. doi:10.1038/nature17042
- Alkharsah KR, Rehman S, Alkhamis F, et al. Comparative and molecular analysis of MRSA isolates from infection sites and carrier colonization sites. *Ann Clin Microbiol Antimicrob*. 2018;17(1):7. doi:10.1186/s12941-018-0260-2
- Alkharsah KR, Rehman S, Alnimir A, et al. Molecular typing of MRSA isolates by spa and PFGE. *J King Saud Univ Sci*. 2019;31(4):999–1004. doi:10.1016/j.jksus.2018.07.018
- Singh S, Rehman S, Fatima Z, et al. Protein kinases as potential anticandidal drug targets. *Front Biosci*. 2020;25:1412–1432.
- Medscape. Cancer to become leading cause of death worldwide by 2010. Available from: <https://www.medscape.com/viewarticle/585098>. Accessed June 15, 2020.

7. The Cancer Atlas. The Burden of Cancer Available from: <https://canceratlas.cancer.org/the-burden/the-burden-of-cancer/>. Accessed June 15, 2020.
8. International Agency for Research on Cancer. Cancer Tomorrow. Available from: <https://gco.iarc.fr/tomorrow/home>. Accessed June 15, 2020.
9. Khan SA, Shahid S, Shahid B, Fatima U, Abbasi SA. Green synthesis of MnO nanoparticles using abutilon indicum leaf extract for biological, photocatalytic, and adsorption activities. *Biomolecules*. 2020;10(5):785. doi:10.3390/biom10050785
10. Ajoudanian N, Nezamzadeh-Ejehieh A. Enhanced photocatalytic activity of nickel oxide supported on clinoptilolite nanoparticles for the photodegradation of aqueous cephalixin. *Mat Sci Semicon Proc*. 2015;36:162–169. doi:10.1016/j.mssp.2015.03.042
11. Khan SA, Arshad Z, Shahid S, et al. Synthesis of TiO<sub>2</sub>/Graphene oxide nanocomposites for their enhanced photocatalytic activity against methylene blue dye and ciprofloxacin. *Compos B Eng*. 2019;175:107120. doi:10.1016/j.compositesb.2019.107120
12. Abbasi A, Sajadi V, Amiri O, et al. MgCr<sub>2</sub>O<sub>4</sub> and MgCr<sub>2</sub>O<sub>4</sub>/Ag nanostructures: facile size-controlled synthesis and their photocatalytic performance for destruction of organic contaminants. *Compos B Eng*. 2019;175:107077. doi:10.1016/j.compositesb.2019.107077
13. Kim SH, Umar A, Kumar R, Ibrahim AA, Kumar G. Facile synthesis and photocatalytic activity of cocoon-shaped CuO nanostructures. *Mater Lett*. 2015;156:138–141. doi:10.1016/j.matlet.2015.05.014
14. Qi X, Su G, Bo G, Cao L, Liu W. Synthesis of NiO and NiO/TiO<sub>2</sub> films with electrochromic and photocatalytic activities. *Surf Coat Technol*. 2015;272:79–85. doi:10.1016/j.surfcoat.2015.04.020
15. Hirpara DG, Gajera HP. Green synthesis and antifungal mechanism of silver nanoparticles derived from chitin- induced exometabolites of *Trichoderma interfusum*. *Appl Organomet Chem*. 2020;34(3):e5407. doi:10.1002/aoc.5407
16. Khan SA, Shahid S, Lee CS. Green synthesis of gold and silver nanoparticles using leaf extract of *clerodendrum inerme*; characterization, antimicrobial, and antioxidant activities. *Biomolecules*. 2020;10(6):835. doi:10.3390/biom10060835
17. Rehman S, Ansari MA, Alzohairy MA, et al. Antibacterial and antifungal activity of novel synthesized neodymium-substituted cobalt ferrite nanoparticles for biomedical application. *Processes*. 2019;7(10):714. doi:10.3390/pr7100714
18. Almessiere MA, Slimani Y, Rehman S, et al. Synthesis of Dy-Y co-substituted manganese-zinc spinel nanoferrites induced anti-bacterial and anti-cancer activities: comparison between sonochemical and sol-gel auto-combustion methods. *Mater Sci Eng C*. 2020;116:111186. doi:10.1016/j.msec.2020.111186
19. Rehman S, Almessiere MA, Tashkandi N, et al. Fabrication of spinel cobalt ferrite (CoFe<sub>2</sub>O<sub>4</sub>) nanoparticles with unique earth element cerium and neodymium for anticandidal activities. *ChemistrySelect*. 2019;4(48):14329–14334. doi:10.1002/slct.201901811
20. Boomi P, Ganesan RM, Poorani G, Prabu HG, Ravikumar S, Jeyakanthan J. Biological synergy of greener gold nanoparticles by using *Coleus aromaticus* leaf extract. *Mater Sci Eng C*. 2019;99:202–210. doi:10.1016/j.msec.2019.01.105
21. EParthiban E, Manivannan N, Ramanibai R, Mathivanan N. Green synthesis of silver-nanoparticles from *Annona reticulata* leaves aqueous extract and its mosquito larvicidal and anti-microbial activity on human pathogens. *Biotechnol Rep*. 2019;21:e00297. doi:10.1016/j.btre.2018.e00297
22. Ijaz F, Shahid S, Khan SA, Ahmad W, Zaman S. Green synthesis of copper oxide nanoparticles using *Abutilon indicum* leaf extract: antimicrobial, antioxidant and photocatalytic dye degradation activities. *Trop J Pharm Res*. 2017;16(4):743–753. doi:10.4314/tjpr.v16i4.2
23. Khan SA, Noreen F, Kanwal S, Iqbal A, Hussain G. Green synthesis of ZnO and Cu-doped ZnO nanoparticles from leaf extracts of *abutilon indicum*, *clerodendrum infortunatum*, *clerodendrum inerme* and investigation of their biological and photocatalytic activities. *Mater Sci Eng C*. 2018;82:46–59. doi:10.1016/j.msec.2017.08.071
24. Lian S, Diko CS, Yan Y, et al. Characterization of biogenic selenium nanoparticles derived from cell-free extracts of a novel yeast *Magnusiomyces ingens*. *3 Biotech*. 2019;9(6):221. doi:10.1007/s13205-019-1748-y
25. Kumar R, Baratto C, Faglia G, Sberveglieri G, Bontempi E, Borgese L. Tailoring the textured surface of porous nanostructured NiO thin films for the detection of pollutant gases. *Thin Solid Films*. 2015;583:233–238. doi:10.1016/j.tsf.2015.04.004
26. Berchmans S, Gomathi H, Rao GP. Electrooxidation of alcohols and sugars catalysed on a nickel oxide modified glassy carbon electrode. *J Electroanal Chem*. 1995;394(1–2):267–270. doi:10.1016/0022-0728(95)04099-A
27. Ezhilarasi AA, Vijaya JJ, Kaviyarasu K, Kennedy LJ, Ramalingam RJ, Al-Lohedan HA. Green synthesis of NiO nanoparticles using *Aegle marmelos* leaf extract for the evaluation of in-vitro cytotoxicity, antibacterial and photocatalytic properties. *J Photochem Photobiol B*. 2018;180:39–50. doi:10.1016/j.jphotobiol.2018.01.023
28. Rehman S, Jermy BR, Akhtar S, et al. Isolation and characterization of a novel thermophile; *Bacillus haysii*, applied for the green synthesis of ZnO nanoparticles. *Artif Cells Nanomed Biotechnol*. 2019;47(1):2072–2082. doi:10.1080/21691401.2019.1620254
29. Rehman S, Jermy R, Asiri SM, et al. Using *Fomitopsis pinicola* for bioinspired synthesis of titanium dioxide and silver nanoparticles, targeting biomedical applications. *RSC Adv*. 2020;10(53):32137–32147. doi:10.1039/D0RA02637A
30. Rehman S, Farooq R, Jermy R, et al. A wild fomes *fomentarius* for biomediation of one pot synthesis of titanium oxide and silver nanoparticles for antibacterial and anticancer application. *Biomolecules*. 2020;10(4):622. doi:10.3390/biom10040622
31. Iqbal J, Abbasi BA, Mahmood T, Hameed S, Munir A, Kanwal S. Green synthesis and characterizations of Nickel oxide nanoparticles using leaf extract of *Rhamnus virgata* and their potential biological applications. *Appl Organomet Chem*. 2019;33(8):e4950. doi:10.1002/aoc.4950
32. US Food & Drug Administration. Detention without physical examination of Stevia leaves, crude extracts of Stevia leaves and foods containing Stevia leaves and/or Stevia extracts. US food and drug administration. 16 august 2019. Import alert 45–06; 2019. Available from: [https://www.accessdata.fda.gov/cms\\_ia/importalert\\_119.html](https://www.accessdata.fda.gov/cms_ia/importalert_119.html). Accessed February 15, 2021.
33. Rajeshwari S, Sevarkodiyone SP. Medicinal properties of *Abutilon indicum*. *Open J Plant Sci*. 2018;3:022–025.
34. Kumar SS, Marella SS, Vipin S, Sharmistha M. Evaluation of analgesic and anti-inflammatory activity of *Abutilon indicum*. *Int J Drug Dev Res*. 2013;5:1402–1407.
35. Tripathi P, Chauhan NS, Patel JR. Anti-inflammatory activity of *Abutilon indicum* extract. *Nat Prod Res*. 2012;26(17):1659–1661. doi:10.1080/14786419.2011.616508
36. Krisanapun C, Lee SH, Peungvicha P, Temsiririrkkul R, Baek SJ. Antidiabetic activities of *Abutilon indicum* (L.) sweet are mediated by enhancement of adipocyte differentiation and activation of the GLUT1 promoter. *Evid Based Complement Alternat Med*. 2011;2011:167684. doi:10.1093/ecam/neq004
37. Srividya AR, Dhanabal SP, Jeevitha S, Varthan VV, Kumar RR. Relationship between antioxidant properties and chemical composition of *Abutilon indicum* Linn. *Indian J Pharm Sci*. 2012;74(2):163–167. doi:10.4103/0250-474X.103854
38. Abdul MM, Sarker AA, Saiful IM, Muniruddin A. Cytotoxic and antimicrobial activity of the crude extract of *Abutilon indicum*. *Int J Pharmacogn Phytochem*. 2011;2:1–4.



39. Bondre AV, Akare SC, Mourya P, Wanjari AD, Tarte PS, Paunikar GV. In vitro cytotoxic activity of leaves of *Abutilon indicum* linn. against ehrlich ascites carcinoma and Dalton's ascitic lymphoma cell line. *RJPP*. 2009;1:72–74.
40. Porchezian E, Ansari SH. Hepatoprotective activity of *Abutilon indicum* on experimental liver damage in rats. *Phytomedicine*. 2005;12(1–2):62–64. doi:10.1016/j.phymed.2003.09.009
41. Paranjhape AN, Mehta AA. A study on clinical efficacy of *Abutilon indicum* in treatment of bronchial asthma. *Orient Pharm Exp Med*. 2006;6:330–335.
42. Rahuman AA, Gopalakrishnan G, Venkatesan P, Geetha K. Isolation and identification of mosquito larvicidal compound from *Abutilon indicum* (Linn.) Sweet. *Parasitol Res*. 2008;102(5):981–988. doi:10.1007/s00436-007-0864-5
43. Shahid S, Khan SA, Ahmad W, Fatima U, Knawal S. Size-dependent bacterial growth inhibition and antibacterial activity of Ag-doped ZnO nanoparticles under different atmospheric conditions. *Indian J Pharm Sci*. 2018;80(01):173–180. doi:10.4172/pharmaceutical-sciences.1000342
44. Khan SA, Rizwan K, Shahid S, Noamaan MA, Rasheed T, Amjad H. Synthesis, DFT, computational exploration of chemical reactivity, molecular docking studies of novel formazan metal complexes and their biological applications. *Appl Organomet Chem*. 2020;34(3):e5444. doi:10.1002/aoc.5444
45. Khan SA, Shahid S, Hanif S, et al. Green synthesis of chromium oxide nanoparticles for antibacterial, antioxidant anticancer, and biocompatibility activities. *Int J Mol Sci*. 2021;22(2):502. doi:10.3390/ijms22020502
46. Hoyo J, Ivanova K, Gaus E, Tzanov T. Multifunctional ZnO NPs-chitosan-gallic acid hybrid nanocoating to overcome contact lenses associated conditions and discomfort. *J Colloid Interface Sci*. 2019;543:114–121. doi:10.1016/j.jcis.2019.02.043
47. Kasprzak MM, Erxleben A, Ochocki J. Properties and applications of flavonoid metal complexes. *RSC Adv*. 2015;5:45853–45877.
48. Singh R, Mendhulkar VD. FTIR studies and spectrophotometric analysis of natural antioxidants, polyphenols and flavonoids in *Abutilon indicum* (Linn) sweet leaf extract. *J Chem Pharm Res*. 2015;7:205–211.
49. Saranya D, Sekar J. GC-MS and FT-IR analyses of ethylacetate leaf extract of *abutilon indicum* (L.) sweet. *Int J Adv Res Biol Sci*. 2016;3:193–197.
50. Kuo PC, Yang ML, Wu PL, et al. Chemical constituents from *Abutilon indicum*. *J Asian Nat Prod Res*. 2008;10(7):689–693.
51. Kannan K, Radhika D, Nikolova MP, Sadasivuni KK, Mahdizadeh H, Verma U. Structural studies of bio-mediated NiO nanoparticles for photocatalytic and antibacterial activities. *Inorg Chem Commun*. 2020;113:107755. doi:10.1016/j.inoche.2019.107755
52. Roy HS, Mollah MY, Islam MM, Susan MA. Poly (vinyl alcohol)–MnO<sub>2</sub> nanocomposite films as UV-shielding materials. *Polym Bull*. 2018;75(12):5629–5643. doi:10.1007/s00289-018-2355-5
53. Ramesh M, Rao MP, Anandan S, Nagaraja H. Adsorption and photocatalytic properties of NiO nanoparticles synthesized via a thermal decomposition process. *J Mater Res*. 2018;33:601–610.
54. Kumar PV, Ahamed AJ, Karthikeyan M. Synthesis and characterization of NiO nanoparticles by chemical as well as green routes and their comparisons with respect to cytotoxic effect and toxicity studies in microbial and MCF-7 cancer cell models. *SN Appl Sci*. 2019;1:1083.
55. Helen SM, Rani MH. Characterization and antimicrobial study of nickel nanoparticles synthesized from dioscorea (Elephant Yam) by green route. *Int J Sci Res*. 2015;4:216–219.
56. Srihasam S, Thyagarajan K, Korivi M, Lebaka VR, Mallem SP. Phytochemical generation of NiO nanoparticles using Stevia leaf extract and evaluation of their in-vitro antioxidant and antimicrobial properties. *Biomolecules*. 2020;10(1):89. doi:10.3390/biom10010089
57. Arianingrum R, Arty IS, Atun S. Synergistic combination of fluoro chalcone and doxorubicin on HeLa cervical cancer cells by inducing apoptosis. *AIP Conf Proc*. 2017;1823:020112.
58. Sadeghi-Aliabadi H, Minaiyan M, Dabestan A. Cytotoxic evaluation of doxorubicin in combination with simvastatin against human cancer cells. *Res Pharm Sci*. 2010;5:127.
59. Nguyen HN, Hoang TM, Mai TT, et al. Enhanced cellular uptake and cytotoxicity of folate decorated doxorubicin loaded PLA-TPGS nanoparticles. *Adv Nat Sci Nanosci*. 2015;6:025005.
60. Umaralikhani L, Jaffar MJ. Antibacterial and anticancer properties of NiO nanoparticles by co-precipitation method. *JOAASR*. 2016;1:24–35.
61. Khan S, Ansari AA, Malik A, Chaudhary AA, Syed JB, Khan AA. Preparation, characterizations and in vitro cytotoxic activity of nickel oxide nanoparticles on HT-29 and SW620 colon cancer cell lines. *J Trace Elem Med Biol*. 2019;52:12–17. doi:10.1016/j.jtemb.2018.11.003

## International Journal of Nanomedicine

### Publish your work in this journal

The International Journal of Nanomedicine is an international, peer-reviewed journal focusing on the application of nanotechnology in diagnostics, therapeutics, and drug delivery systems throughout the biomedical field. This journal is indexed on PubMed Central, MedLine, CAS, SciSearch®, Current Contents®/Clinical Medicine,

Submit your manuscript here: <https://www.dovepress.com/international-journal-of-nanomedicine-journal>

Dovepress

Journal Citation Reports/Science Edition, EMBase, Scopus and the Elsevier Bibliographic databases. The manuscript management system is completely online and includes a very quick and fair peer-review system, which is all easy to use. Visit <http://www.dovepress.com/testimonials.php> to read real quotes from published authors.